ENVIRONMENTAL RESEARCH
LETTERS

LETTER • OPEN ACCESS

Where the past meets the present: connecting nitrogen from watersheds to streams through groundwater flowpaths

To cite this article: Eric M Moore *et al* 2023 *Environ. Res. Lett.* **18** 124039

View the article online for updates and enhancements.

You may also like

- Wind-modulated groundwater discharge along a microtidal Arctic coastline
Julia A Guimond, Cansu Demir, Barret L Kurylyk et al.
- A model comparison assessing the importance of lateral groundwater flows at the global scale
Inge E M de Graaf and Kerstin Stahl
- Using multiple tracers to quantify groundwater discharge to Yellow river in Weining plain
Y S Wang, X X Chen, M N Zhang et al.

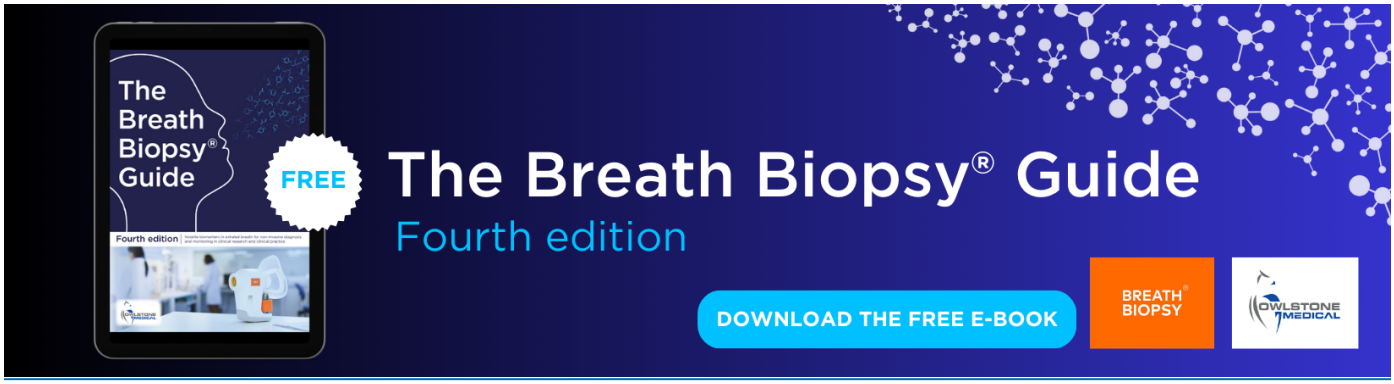

This content was downloaded from IP address 137.99.143.9 on 07/12/2023 at 15:11

IOP Publishing Environ. Res. Lett. 18 (2023) 124039 https://doi.org/10.1088/1748-9326/ad0c86

ENVIRONMENTAL RESEARCH
LETTERS

OPEN ACCESS

RECEIVED
12 May 2023

REVISED
16 October 2023

ACCEPTED FOR PUBLICATION
14 November 2023

PUBLISHED
23 November 2023

Original content from this work may be used under the terms of the Creative Commons Attribution 4.0 licence.

Any further distribution of this work must maintain attribution to the author(s) and the title of the work, journal citation and DOI.

LETTER

Where the past meets the present: connecting nitrogen from watersheds to streams through groundwater flowpaths

Eric M Moore[1,*], Janet R Barclay[2], Adam B Haynes[1,5], Kevin E Jackson[1], Alaina M Bisson[1], Martin A Briggs[3] and Ashley M Helton[1,4]

[1] Department of Natural Resources and the Environment, University of Connecticut, Storrs, CT, United States of America
[2] U.S. Geological Survey, New England Water Science Center, U.S. Geological Survey, East Hartford, CT, United States of America
[3] U.S. Geological Survey, Hydrologic Remote Sensing Branch, Storrs, CT, United States of America
[4] Center for Environmental Science and Engineering, University of Connecticut, Storrs, CT, United States of America
[5] Currently at Earth and Planetary Sciences Department, University of California Santa Cruz, Santa Cruz, CA, United States of America
[*] Author to whom any correspondence should be addressed.

E-mail: eric.m.moore@uconn.edu

Keywords: groundwater discharge, nitrate, land use, contributing area, MODPATH

Supplementary material for this article is available online

Abstract

Groundwater discharge to streams is a nonpoint source of nitrogen (N) that confounds N mitigation efforts and represents a significant portion of the annual N loading to watersheds. However, we lack an understanding of where and how much groundwater N enters streams and watersheds. Nitrogen concentrations at the end of groundwater flowpaths are the culmination of biogeochemical and physical processes from the contributing land area where groundwater recharges, within the aquifer system, and in the near-stream riparian area where groundwater discharges to streams. Our research objectives were to quantify the spatial distribution of N concentrations at groundwater discharges throughout a mixed land-use watershed and to evaluate how relationships among contributing and riparian land cover, modeled aquifer characteristics, and groundwater discharge biogeochemistry explain the spatial variation in groundwater discharge N concentrations. We accomplished this by integrating high-resolution thermal infrared surveys to locate groundwater discharge, biogeochemical sampling of groundwater, and a particle tracking model that links groundwater discharge locations to their contributing area land cover. Groundwater N loading from groundwater discharges within the watershed varied substantially between and within streambank groundwater discharge features. Groundwater nitrate concentrations were spatially heterogeneous ranging from below 0.03–11.45 mg-N/L, varying up to 20-fold within meters. When combined with the particle tracking model results and land cover metrics, we found that groundwater discharge nitrate concentrations were best predicted by a linear mixed-effect model that explained over 60% of the variation in nitrate concentrations, including aquifer chemistry (dissolved oxygen, Cl^-, SO_4^{2-}), riparian area forested land cover, and modeled physical aquifer characteristics (discharge, Euclidean distance). Our work highlights the significant spatial variability in groundwater discharge nitrate concentrations within mixed land-use watersheds and the need to understand groundwater N processing across the many spatiotemporal scales within groundwater cycling.

1. Introduction

Nitrogen (N) applied to land surfaces infiltrates with groundwater recharge and has substantially increased N concentrations in aquifers over the last century (Galloway and Cowling 2002, Puckett *et al* 2011, Houlton and Morford 2014). Groundwater N discharge to streams represents a widespread nonpoint source of N that can be significantly delayed from terrestrial applications based on varying groundwater transit times (Tesoriero *et al* 2013, Stets *et al* 2020) causing groundwater legacies to confound surface

© 2023 The Author(s). Published by IOP Publishing Ltd

water quality management (Rosenberry *et al* 2016, Liu *et al* 2017, Vero *et al* 2018). Although groundwater N is known to be a substantial component of N loading to streams (Johnson and Stets 2020, Wherry *et al* 2021), we lack the ability to predict the spatial distribution of groundwater N loading to streams, hindering mitigation efforts (Sanford and Pope 2013, Van Meter *et al* 2018).

Groundwater N loading to streams depends on complex biogeochemical interactions across space and time (Rivett *et al* 2008). Nitrogen deposition on land surfaces is often heterogeneous, and N may undergo multiple transformations before entering surface water (Kaushal *et al* 2011, Kolbe *et al* 2019). Initially, some N is retained by vegetation and soil through biological and physical processes (Fowler *et al* 2013). Subsequently, the fate of N percolating to aquifers is controlled by groundwater residence times, redox gradients, and electron donor availability along groundwater flowpaths (Ocampo *et al* 2006, Kolbe *et al* 2019, Tesoriero *et al* 2021, Henri and Harter 2022). As groundwater interfaces with surface water at the end of flowpaths, organic carbon within the river corridor may promote further N processing through denitrification, the microbially mediated reduction of nitrate to nitrous oxide or nitrogen gas (Lutz *et al* 2020). Riparian buffers and reducing N application mitigate loading to surface waters (Ranalli and Macalady 2010). However, the effects of best management practices are not always realized downstream (Chang *et al* 2021, Martin *et al* 2021) and in some cases, riparian buffers can create preferential flowpaths that allow N to bypass management practices (Hester and Fox 2020).

Groundwater N is transported from the land surface along groundwater flowpaths to surface waters. Groundwater flowpaths form in response to recharge patterns, surface and bedrock topography, and hydraulic conductivity (Winter *et al* 1998). However, identifying where flowpaths interface with surface water throughout a stream network is challenging. Field mapping of groundwater discharge at broad scales is difficult due to access to continuous reaches and time-intensive field methods (Harvey and Wagener 2000, Rosenberry *et al* 2021). Predicting groundwater discharge locations based on subsurface characteristics is limited by the spatial resolution and accuracy of existing datasets (e.g. SSURGO, Nauman *et al* 2014), and is further complicated by land use (Scanlon *et al* 2005), which can disconnect groundwater from surface water.

Groundwater models can be used to predict where groundwater discharges, but field validation is challenging because of the significant heterogeneity in how groundwater is expressed along streams in terms of discharge, spatial distribution, and lateral extent (Briggs *et al* 2021, Barclay *et al* 2022). Thermal infrared (TIR) cameras can be used to map groundwater discharge from the point-to-reach scale (Dugdale *et al* 2015, Hare *et al* 2017, Sullivan *et al* 2021) and have recently been used to evaluate modular finite difference flow model (MODFLOW)-predicted discharge locations (Barclay *et al* 2022). In this study, we integrate high-resolution groundwater discharge TIR surveys and biogeochemical sampling with a particle tracking model to spatially connect groundwater discharge to its contributing land area and physical aquifer characteristics. Reducing the uncertainty of groundwater N inputs represents a critical knowledge gap for building more resilient riverscapes, particularly as streams face further human-induced changes (Wherry *et al* 2021).

We hypothesized that spatial variation in groundwater NO_3^- concentrations is a function of (1) land cover contributing to groundwater flowpaths, (2) physical characteristics that describe water movement through the aquifer (3) groundwater chemistry representing reactivity along flowpaths, and (4) riparian characteristics controlling biogeochemical processing along and at the end of groundwater flowpaths (figure 1). The goal of this study is to quantify the spatial patterns of N in groundwater discharges throughout a mixed land-use stream network. Our objectives were to (1) map the spatial variation of groundwater discharge N concentrations, and (2) evaluate the relationships between groundwater discharge N concentrations and groundwater chemistry, modeled aquifer characteristics, and contributing area and riparian land cover.

2. Methods

2.1. Study area

The Farmington River watershed (1572 km^2) is a fifth-order tributary of the Connecticut River located in Connecticut and Massachusetts, USA. It is predominantly forested (67%) with development (18%), agriculture (3%), and grassland (1%) primarily along the mainstem and forested wetlands (8%) and open water (3%) throughout the watershed (Dewitz and U.S. Geological Survey 2021, figure 2). Bedrock geology consists of New England crystalline rock, Mesozoic sandstone, and Newark Supergroup basalt, which is overlain by coarse-grained, stratified glacial deposits in the lower portion of the watershed while the upper portion consists of fine-grained, unstratified glacial till (Olcott 1995). Bedrock depth along the mainstem is 23.2 m $\pm$ 5.5 m (Jackson *et al* 2023) and mean saturated hydraulic conductivity is 9.3 m d^{-1} (Briggs *et al* 2021). The daily mean discharge is 30.9 m^3 s^{-1} (USGS NWIS, gage 01189995, 2010–2022).

2.2. Field surveys of groundwater discharge

We used handheld TIR cameras (FLIR, Wilsonville, OR) to identify areas of groundwater discharge along streambanks (Deitchman and Loheide 2009,

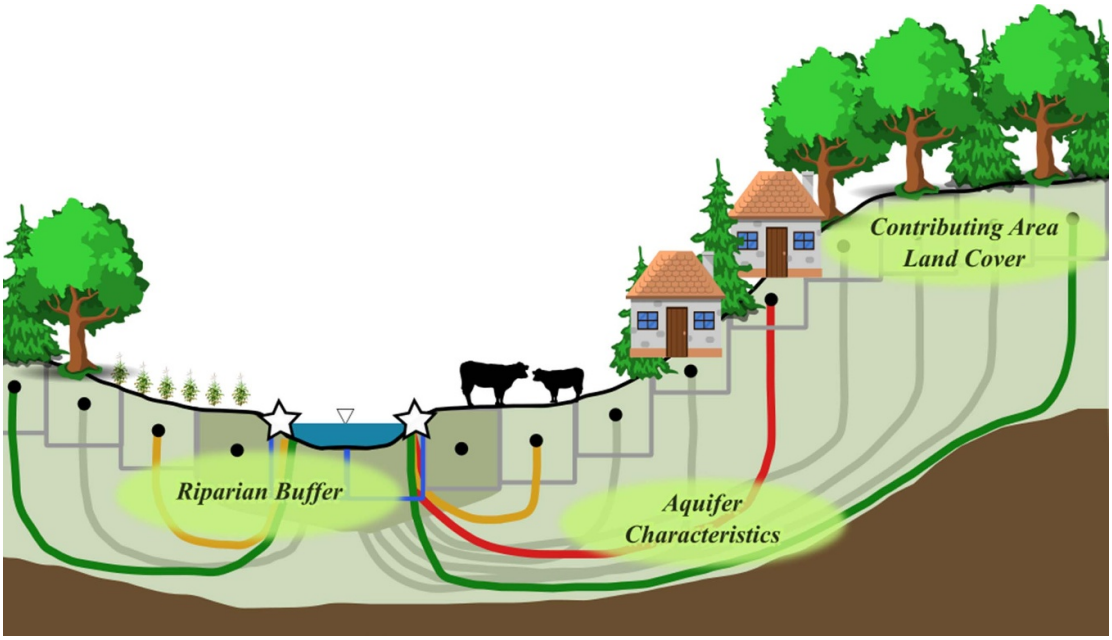

Figure 1. Conceptual model linking zones along groundwater flowpaths where controls of nitrogen removal are expected to vary—upon recharge in contributing areas, within the aquifer, and riparian area and near-stream sediments—with particle tracking model structure. Gray squares with black points represent particle tracking model cells with groundwater flowpath lines colored by representative contributing area land cover. Blue squares near the stream represent locations of predicted groundwater discharge. Groundwater discharge sampling locations are shown with a white star.

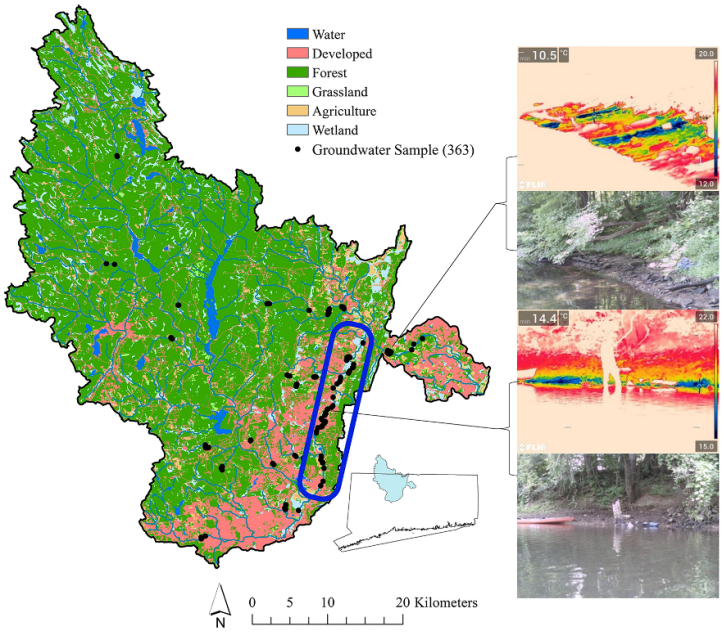

Figure 2. The Farmington River watershed. Sampled groundwater discharges are shown as black circles ($n = 363$). The mainstem 25 km reach is highlighted with a blue box. The right panel shows two groundwater discharge faces with coincident thermal and real-color images where regions of red and white are near air temperature and blue regions are cold groundwater discharging along the river. Images by Eric Moore 8/2022.

Briggs and Hare 2018, Barclay *et al* 2022). Following Barclay *et al* (2022) and Briggs *et al* (2021), we surveyed streams via wading and canoeing to map groundwater discharges at the meter scale along 36 stream reaches totaling over 60 km from 2017 and 2019–2020. Surveys were completed during baseflow (July–November, <30.9 m^3 s^{-1}) when surface water temperatures were above 15 °C and warmer than discharging groundwater (figure 2). Groundwater discharges were characterized using GPS coordinates, TIR, and direct temperature and lateral extent measurements. We identified over 300 unique groundwater discharges ranging from 1 m to over 200 m in lateral extent (Moore *et al* 2020, Barclay *et al* 2022).

2.3. Sample collection

We quantified chemical and spatial variability of groundwater chemistry by sampling mapped groundwater discharge locations (2017, 2019–2021). Because groundwater flux rates within discharge features can vary significantly (Haynes *et al* 2023), we collected our samples from the coldest point assuming this was the most representative sample of groundwater flow through the streambank. We used push-point samplers (MHE Products, East Tawas, MI) inserted 20 cm, or until resistance, into the sediment ($n = 363$). We sampled previously mapped groundwater discharges along 25 km of the 5th-order mainstem and 19 small streams (figure 2). Along the mainstem, we randomly chose locations to sample ($n = 107$) and sampled as many groundwater discharge locations as possible in smaller streams ($n = 123$). Groundwater was pulled through the push-point sampler and purged until it ran clear before sample collection. We measured specific conductance, temperature, and dissolved oxygen (DO) *in situ* using a calibrated YSI-6000 (YSI Inc., Yellow Springs, OH). Groundwater was collected to analyze nitrate (NO_3^-), ammonia (NH_4^+), total dissolved nitrogen (TDN), chloride (Cl^-), sulfate (SO_4^{2-}), and dissolved organic carbon (DOC) in acid-washed and field-rinsed HDPE bottles. We quantified dissolved nitrogen gas (N_2), a proxy for denitrification (Böhlke *et al* 2002, Kennedy *et al* 2009) following Lamberti and Hauer (2017), and nitrous oxide (N_2O) following Helton *et al* (2014). Coincident surface water samples were collected (1–2 per sampling day). Additional details on sample treatment and analysis can be found in Moore *et al* (2023) and supplemental information (SI).

2.4. Particle tracking model

Groundwater discharge locations throughout the network were estimated using a MODPATH particle tracking model (Pollock 2012), which tracks hypothetical water particles through an aquifer based on the outputs of a MODFLOW groundwater model (Niswonger *et al* 2011). We used an existing model (Barclay *et al* 2020b, model name: *RivK_BedK_drn*) with 250,000 particles across a 300 m^2 grid. Particles were distributed to starting cells ($n = 18{,}113$) based on recharge rate (Reitz *et al* 2017) and were tracked from the model start cell on the land surface to model end cells ($n = 2998$) along the network with unique flowpath lines. Modeled aquifer characteristics were generated for each model end cell discharging along the network, including median residence time (years), median Euclidean distance (m), maximum flowpath depth (m), and median groundwater discharge per reach length ($m^3\ m^{-1}$). Additional details on model implementation can be found in SI and Barclay *et al* (2020a), (2020b).

2.5. Riparian and contributing area land cover

We evaluated watershed land cover from 2001 to 2019 finding minimal change (forest −1.47%, developed +1.30%, agriculture −0.38%, wetland +0.38%, grassland +0.61%, water −0.43%); therefore, we opted to use the 2019 National Land Cover Dataset (Dewitz and U.S. Geological Survey 2021). We combined NLCD classes into forest (gridcodes 41–43), developed (21–31), agriculture (81–82), wetland (90–95), grassland (51–74), and water (11–12) (figure 2). Because fertilizer application rates are only available at the county-scale (Byrnes *et al* 2020), we used percent land cover as a proxy for anthropogenic nitrogen sources. We also accounted for anthropogenic N sources by calculating the density of people on septic. We created a spatial data layer representing where people are most likely to dwell in homes with septic systems, or 'settled land', by using a 150 m buffer of developed (low density, medium density, and open space) classes of the 1996 C-CAP land cover (NOAA 2022). We paired 'settled land' with the number of people on septic systems reported in the 1990 census (U.S. Census Bureau 1990) by dividing the number of people on septic in each census block by the area of 'settled land' in each census block. The result is a septic density value for 'settled land' in each census block. We estimated percent land cover and septic density for the riparian area using a 300 m buffer radius around each sampling location.

We also estimated percent land cover and septic density for the land area contributing groundwater to each groundwater discharge sampling location (i.e. contributing area). We discretized the area of each 2019 land cover class and septic density for each MODPATH model start cell. For each model end cell along the stream network, we traced all particles transported to that end cell back to their start cells. The group of start cells connected to a model end cell make up that end cell's contributing area. We then calculated the weighted average land cover based on the number of particles connecting each starting cell to the end cell. Thus, we connected sampling locations to the weighted average contributing area land cover supplying recharge. The contributing area to a groundwater discharge location includes all land surface cells connected by groundwater flow paths, regardless of their hydrologic connection via surface topography. Spatial analyses were performed using ArcMap (ESRI 2021 Inc., Redlands, CA).

2.6. Linear mixed-effects models of groundwater NO_3^-

We conducted five linear mixed-effects model selections based on four sets of predictor variables that represent the major drivers of discharging NO_3^- concentrations: (1) contributing area weighted percent forest, wetland, and agriculture, and density of people on septic, (2) simulated residence time, Euclidean

distance traveled, flowpath depth, and groundwater discharge rate, (3) measured DO, SO_4^{2-}, Cl^-, and DOC concentrations in groundwater (representative of aquifer biogeochemistry), and (4) riparian area percent forest, wetland, and agriculture, and density of people on septic. We used sampling year as a random effect to account for differences in the annual flow regime because 2021 had consistently higher river discharge due to three hurricanes. Percent forest and developed land cover were highly correlated (Pearson's $r = -0.92$ for contributing area and -0.53 for riparian area) therefore we opted to exclude developed land cover. Model selection was performed through an exhaustive search of all model variables. Best fit models were selected as those with the lowest Bayesian information criterion and highest model weight (table S1). We also conducted model selection for the combined categories of variables including only those variables within the best-fit models of the first four model selections. In summary, we conducted four individual sets of models (contributing area, aquifer characteristics, groundwater biogeochemistry, and riparian buffer) and one combined model using the best fit model from each individual model set. Variables were $\log_{10}$ transformed to meet assumptions of normality (Shapiro–Wilks, $p < 0.05$). Statistical analyses were performed using R 4.1.2 (R Core Team 2021).

3. Results

3.1. Spatial patterns of N at groundwater discharges

Groundwater N was heterogeneous throughout the watershed (figure 3). Groundwater collected only meters apart often varied substantially; for example, at river km 22, NO_3^- decreased from 7.42 to 0.37 mg-N/L within 30 m. TDN and NO_3^- were highly correlated across the watershed (rho = 0.937, $p < 0.05$, figure S1), and NO_3^- constituted over 90% of TDN, indicating that most of the N sampled was NO_3^-. We generally observed low NH_4^+ along the 25 km reach, yet there were rare locations with NH_4^+ up to 2 mg l^{-1}, and NH_4^+ was negatively correlated with NO_3^- (rho = -0.28, $p < 0.05$). Small stream concentrations and ranges of NO_3^- and NH_4^+ in streams were lower than the mainstem (table 1), reflecting the shift from predominantly forest to mixed land use.

Denitrification end-products also varied considerably, indicating heterogeneity in N processing. Mainstem N_2O was positively correlated with NO_3^- (rho = 0.58, $p < 0.05$) whereas excess N_2, our surrogate measure of denitrification, was not (rho = -0.03, $p > 0.05$). Small stream N_2O and N_2 groundwater concentrations were significantly lower than mainstem concentrations and N_2O was positively correlated with NO_3^- (rho = 0.66, $p < 0.05$), whereas N_2 was not (rho = 0.02, $p > 0.05$). Only 60% of N_2 samples contained excess N_2 from complete denitrification. DO varied considerably across the 25 km reach, indicating significant redox gradient heterogeneity within the aquifer (Tesoriero *et al* 2021). A laterally extensive groundwater face near river km 11 contained DO ranging from 1.35 to 6.07 mg l^{-1} within 150 m (figure 3). Mainstem and small stream DO were not significantly different but were positively correlated with NO_3^- (mainstem rho = 0.49, $p < 0.05$; small stream rho = 0.28, $p < 0.05$).

We also collected other geochemical variables that may influence groundwater N cycling. DOC concentrations were generally low (median: 0.85 mg l^{-1}) and were not correlated with NO_3^- along the mainstem (rho = -0.19, $p > 0.05$) or small streams (rho = -0.02, $p > 0.05$). Mainstem DOC was significantly higher than headwaters (table 1). Sulfate concentrations were significantly higher along the mainstem than small streams, and SO_4^{2-} was positively correlated with NO_3^- along the mainstem (rho = 0.32, $p < 0.05$) and small streams (rho = 0.30, $p < 0.05$). Chloride concentrations were also heterogeneous ranging from 2.04 to 2337.84 mg l^{-1} along the mainstem and 0.03–123.31 mg l^{-1} in small streams. Sediment grab samples show that over 90% of the sediment was sand or larger grain size (Moore *et al* 2023). Organic matter ranged from 0.2 to 13.34% along the mainstem and 0.2%–73.91% in small streams.

3.2. Particle tracking model

Particle tracking applied to a calibrated groundwater flow model from Barclay *et al* (2020b) spatially connected our samples to contributing area land cover. Across the entire watershed, modeled groundwater flowpath characteristics were generally consistent with model predictions at sampling locations (SI). MODPATH particles terminated at 242 of the 363 sampling locations. The remaining 121 samples occurred along reaches that were not predicted to receive particles, particularly in 1st and 2nd order streams (figure 4). Modeled flowpath characteristics increased with stream order (figure S2). At sampling locations, groundwater residence times ranged from 0.1 to 406.7 years (median 9.2 years) and the maximum flowpath depth ranged from 0.7 to 183.6 m (median = 96.0 m). Euclidean distance to sampling locations ranged from 150.0–3400.8 m (median = 1006.1 m) and median groundwater discharge rates ranged from 3×10^{-3} to 18.8 m^3 m^{-1} (median = 3.8 m^3 m^{-1}).

3.3. Predicting spatial patterns of groundwater NO_3^-

The model that best explained groundwater discharge NO_3^- concentrations included variables that describe

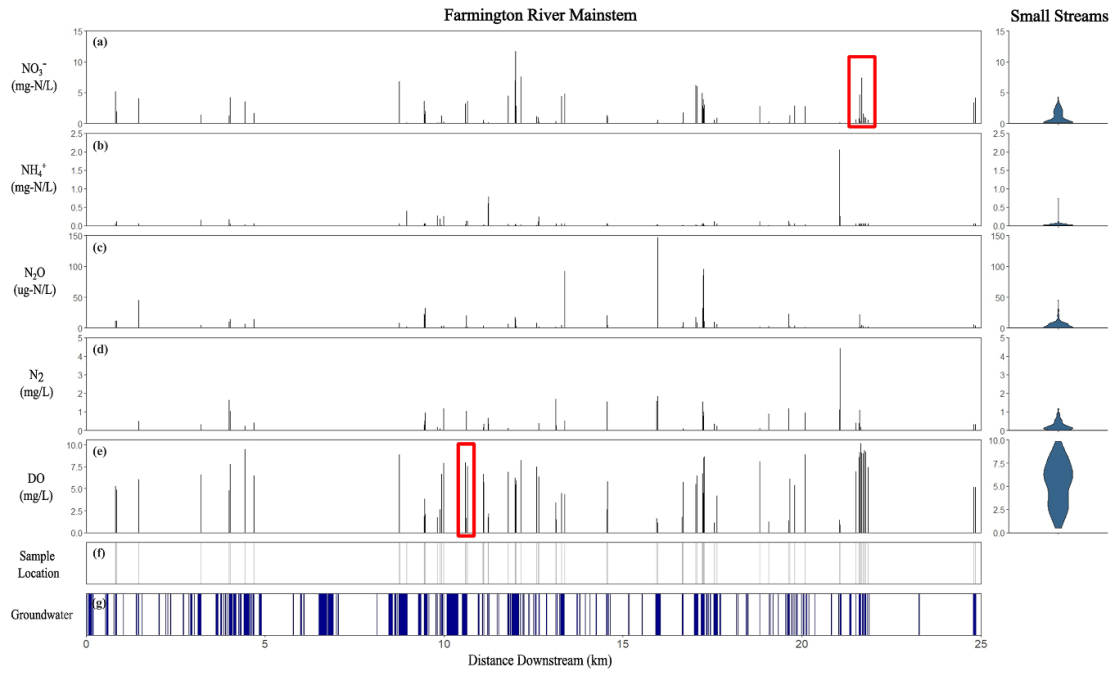

Figure 3. Longitudinal groundwater discharge sampling along the mainstem Farmington River, CT, USA. The blue lines on the bottom panel (g) represent the longitudinal extent of mapped groundwater discharges. Gray lines in panel (f) represent the subset of groundwater discharge locations sampled for chemistry. Red boxes highlight examples of areas where solute concentrations vary dramatically over short distances. Violin plots of small stream groundwater discharge concentrations are shown on the right for comparison.

riparian land cover, aquifer biogeochemistry, and modeled groundwater discharge and flowpath distance (table 2). Aquifer biogeochemistry and riparian land cover variables were the strongest individual group of predictors of NO_3^- (R^2 = 0.41 and 0.32 respectively, table 2). Concentrations of DO, SO_4^{2-}, and Cl^- were positively correlated with NO_3^-. Riparian and contributing area forest cover were both negatively related to NO_3^-, though contributing area forest cover was not included in the best-performing model. Interestingly, riparian agricultural land cover did not correlate with groundwater NO_3^- and was not selected through model subsetting (table S1). However, the density of people on septic systems is an influential variable within the riparian area. Aquifer characteristics derived from particle tracking predicted groundwater NO_3^- to increase with increased discharge and decrease with distance traveled but explained relatively little variation (R^2 = 0.15). Contributing area land cover was not a significant parameter within the full model selection indicating that flowpath characteristics and biogeochemistry convolute connections between discharging groundwater NO_3^- patterns and contributing area land cover.

We accounted for flow year as a random effect resulting in increased predictive power in all models except the riparian area model indicating that sampling year flow condition was an influential variable in predicting groundwater NO_3^- concentrations (table 2). Groundwater NO_3^- and NH_4^+ were elevated and more heterogeneous during the 2019 low-flow year than the 2021 high-flow year and indicators of denitrification (N_2O and N_2) were also more variable during the 2019 low-flow year (figure S3).

4. Discussion

Our research shows that groundwater discharge N concentrations are highly heterogeneous both within and among streambank discharge features, and that NO_3^- concentrations are best predicted by (1) aquifer biogeochemistry, (2) riparian area forest cover and density of people on septic, and (3) flowpath distance and groundwater discharge rate. Contrary to our expectation, we found that contributing area land cover was not a major predictor of groundwater NO_3^-. This contrasts prior studies that have directly linked surface land cover to groundwater well N concentrations (Lockhart *et al* 2013), baseflow N concentrations in streams (Johnson and Stets 2020), and groundwater discharge N concentrations (Cole *et al* 2006, Shabaga and Hill 2010). These studies were conducted along comparatively short riparian flowpaths, where groundwater N concentrations are currently elevated due to contemporary N application. Within our study watershed attempts to link contributing area land cover to groundwater discharge N concentrations were likely complicated by heterogeneous N inputs from mixed land uses and differential N processing along flowpaths.

Table 1. Groundwater discharge solute concentrations along the mainstem of the Farmington River, CT, and small streams. Bolding indicates significant differences of medians between mainstem and small stream groundwater chemical samples (Wilcoxon, $p < 0.05$). Counts (n) represent any chemical data missed during sample collection. Concentrations below detection are listed as n.d. (non-detect). Nitrate (NO_3^-), ammonia (NH_4^+), total dissolved nitrogen (TDN), chloride (Cl^-), sulfate (SO_4^{2-}), dissolved oxygen (DO), dissolved organic carbon (DOC), dissolved nitrogen gas (N_2), nitrous oxide (N_2O).

		Farmington River mainstem	Small streams
NO_3^- (mg-N/L)	Median:	**1.1**	**0.49**
	Range:	n.d.—11.65	n.d.—4.34
	Std. error:	0.25	0.09
	n:	107/107	123/123
NH_4^+ (mg-N/L)	Median:	**0.05**	**0.03**
	Range:	0.01–2.05	0.02–0.74
	Std. error:	0.03	0.01
	n:	107/107	123/123
N_2O (ug-N/L)	Median:	**3.83**	**3.78**
	Range:	n.d.—146.41	n.d.—45.32
	Std. error:	2.02	0.59
	n:	97/107	123/123
N_2 (mg l^{-1})	Median:	**0.34**	**0.15**
	Range:	n.d.—4.42	n.d.—1.17
	Std. error:	0.08	0.04
	n:	106/107	123/123
DO (mg l^{-1})	Median:	5.16	5.68
	Range:	0.1–10.55	0.49–10.56
	Std. error:	0.28	0.22
	n:	101/107	123/123
DOC (mg l^{-1})	Median:	**0.84**	**0.73**
	Range:	n.d.—3.63	0.31–2.40
	Std. error:	0.07	0.03
	n:	107/107	123/123
SO_4^{2-} (mg-S/L)	Median:	**3.55**	**2.89**
	Range:	0.12–52.57	0.50–12.88
	Std. error:	0.76	0.20
	n:	107/107	123/123
Cl^- (mg l^{-1})	Median:	**27.5**	**19.63**
	Range:	n.d.—2337.84	n.d.—123.31
	Std. error:	23.62	2.33
	n:	107/107	123/123

Throughout the watershed, groundwater well NO_3^-concentrations ranged from non-detect to 9.8 mg-N/L (median = 0.83 mg-N/L, n = 90, 1953–2017, USGS NWIS) and are consistent with our groundwater discharge NO_3^- data (table 1). Groundwater well NO_3^- concentrations show little change over time (figure S4) indicating that while our study watershed contains historic agriculture (Jenkins 1925) groundwater N is not consistently elevated. Spatial variation in N application, including lawn and agricultural fertilizers and septic drainage, may drive areas of high groundwater NO_3^-. For example, high groundwater NO_3^- concentrations were found along the mainstem surrounded by golf courses and agricultural fields.

The extensive chemical heterogeneity in discharging groundwater (figure 3) suggests high uncertainty in predicting groundwater N loading to streams across the watershed. For example, we located approximately 4000 m of streambank groundwater discharge along the mainstem that extended approximately 0.5 m vertically up the streambank (Haynes *et al* 2023). When we use the 5th (0.078 mg-N/L) and 95th (5.12 mg-N/L) percentile of groundwater discharge NO_3^- concentrations and estimate groundwater flux to be 0.5 m d^{-1} (Haynes *et al* 2023), groundwater NO_3^- load ranges from 6740 to 442,360 kg d^{-1}. Estimating surface water NO_3^- load from the mainstem using our 5th (0.78 mg-N/L) and 95th (1.92 mg-N/L) percentile surface water NO_3^- concentrations and mean daily river discharge (30.9 cms) results in a daily surface water load of 208–5,125 kg d^{-1} of NO_3^-. These estimates indicate that groundwater is the primary source of N loading

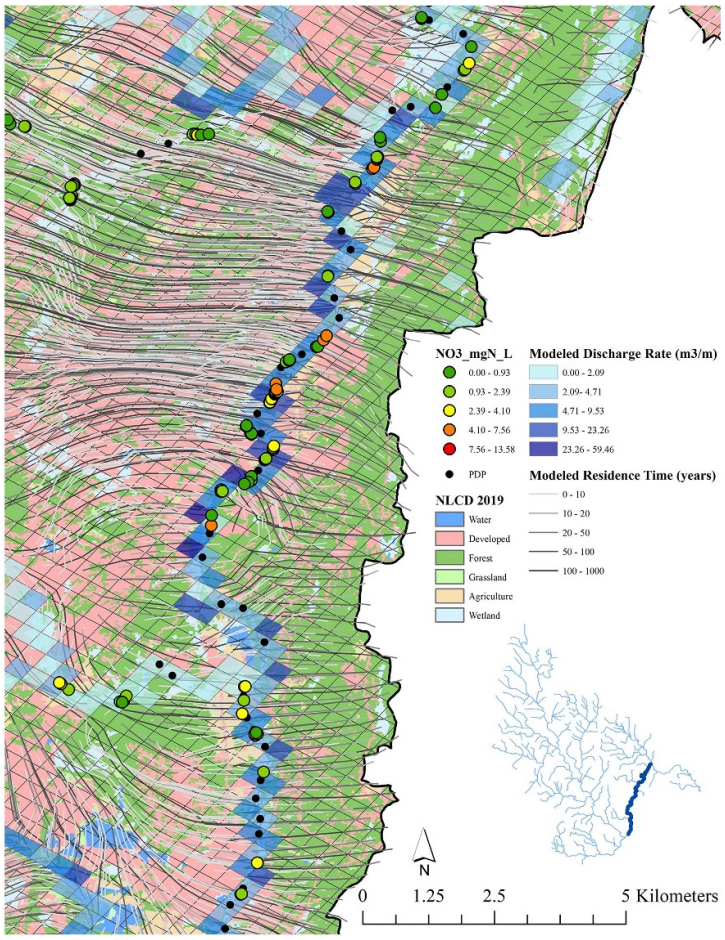

Figure 4. Particle tracking model flowpath lines along the mainstem of the Farmington River, CT overlain on 2019 National Land Cover Dataset. Gray to black lines represent predicted particle residence time from recharge to discharge. Blue boxes show modeled groundwater discharge rates along the river network. Black points represent not sampled streambank discharge locations, while colored points indicate sampled groundwater discharge NO_3^- concentrations.

Table 2. Coefficients for best fit linear mixed-effects models for groundwater discharge nitrate (NO_3^-) concentrations in the Farmington River, CT, USA. Dependent variables are shown on the left with coefficients and significance (* indicates $p < 0.05$) of each best fit model. Detailed model selection and regression output is included in SI (table S1).

	$\log(NO_3^-)$				
	Contributing area	Flowpath	Biogeochemistry	Riparian area	Full model
Weighted % forest	−0.03*	—	—	—	—
Weighted % agriculture	0.05*	—	—	—	—
$\log$(Discharge)	—	0.49*	—	—	0.21*
$\log$(Median distance)	—	−0.46*	—	—	−0.36*
$\log$(DO)	—	—	0.71*	—	0.71*
$\log(SO_4^{2-})$	—	—	0.79*	—	0.64*
$\log(Cl^-)$	—	—	0.36*	—	0.17*
Buffer % forest	—	—	—	−0.03*	−0.02*
Buffer septic	—	—	—	0.01*	0.003*
Constant	0.95*	2.16*	−3.60*	0.17	−0.12
Model weight	0	0	0	0	1
Conditional R^2	0.20	0.17	0.52	0.32	0.63
Marginal R^2	0.17	0.15	0.41	0.32	0.57
Observations	239	239	239	239	239
Log likelihood	−432.00	−436.78	−385.01	−411.91	−351.92
Bayesian Inf. Crit.	891.38	900.93	802.88	851.20	758.61

within our study watershed, highlighting the challenge of empirically quantifying groundwater N contribution within entire watersheds (Mulholland *et al* 2008) and the importance of in-stream N retention and removal in surface waters as shown by significantly less N flux in surface waters versus groundwaters (Wollheim *et al* 2006, Mullholand *et al* 2008). Groundwater discharge N also varied significantly between sampling years where NO_3^- concentrations were lower during the high (2021) versus low (2019, 2020) flow years, suggesting that annual variability in groundwater discharge N must also be considered when budgeting N loading from groundwater (figure S3).

Connecting individual groundwater flowpaths from their point of discharge back to surface land use is impossible with empirical methods; therefore, we used a novel integration of field-collected samples and flowpath modeling to connect discharging groundwater chemistry back to contributing land areas. Like Barclay *et al* (2022) we were able to accurately predict relative groundwater discharge patterns along 3rd and 5th-order streams but struggled to predict discharge in smaller streams (figure 4). Of the 363 groundwater samples collect only 66% of them were predicted to receive particles by the MODPATH model limiting our understanding of how contributing area land cover affects groundwater N concentrations at the river network scale. Modeled flowpath characteristics varied by stream order with 3rd and 5th receiving higher discharge from longer and deeper flowpaths (figure S2). We related predicted locations of groundwater discharge back to their land cover source. However, it did not allow us to generate concrete conclusions about the fate of N from the contributing area, particularly in small streams. This may be due to model resolution; future modeling efforts may consider finer, or even flexible, spatial resolutions to better predict groundwater discharge in small streams. Equally plausible is that reactivity along the groundwater flowpaths could be obscuring the relationship between discharge chemistry and contributing land area (Rivett *et al* 2008).

Rates of N removal along groundwater flowpaths are typically elevated upon infiltration and at the terminal ends of flowpaths where organic carbon availability is often high (Gorski *et al* 2022). N removal rates can also be high within aquifers if conditions are appropriate for denitrification (Rivett *et al* 2008, Kolbe *et al* 2019, Henri and Harter 2022). Our groundwater discharge samples were low in DOC due to a lack of calcareous bedrock (Olcott 1995), and we found low sediment organic matter at sampling locations, limiting carbon-based denitrification. We found elevated SO_4^{2-} within discharging groundwater suggesting potential for sulfur-fueled denitrification within the aquifer (Megonigal *et al* 2003, Ben Maamar *et al* 2015). We also found evidence of denitrification along groundwater flowpaths (figure 3: N_2O and N_2) consistent with other groundwater studies (Tesoriero *et al* 2000, Hinshaw *et al* 2020, McAleer *et al* 2017, Chen *et al* 2014), however only N_2O was strongly related to NO_3^- concentrations ($R^2 = 0.51$, $p < 0.05$). Low NH_4^+ coinciding with elevated DO and SO_4^{2-} suggest that nitrification (Ward 2008) and sulfur denitrification (Hayakawa *et al* 2021) could lead to elevated NO_3^- and N_2O in discharging groundwater. Most of our groundwater DO samples were above the 2 mg l^{-1} anoxic threshold for denitrification (Rivett *et al* 2008). High groundwater DO concentrations support our finding that only 60% of samples contained excess N_2 indicating conditions favorable for incomplete rather than complete denitrification.

Low DOC, sub-oxic groundwater, and short residence times within the watershed likely created heterogeneous patterns of N removal and constrained reduction of NO_3^-. However, our physical methods could have biased this interpretation; we identified preferential discharges, which by definition have relatively high flux rates that reduce N attenuation potential (Ocampo *et al* 2006, Briggs and Hare 2018). We did not sample more diffuse groundwater discharge, which may have lower groundwater flux rates but longer residence times and higher rates of biogeochemical reactivity. Even so, our results are consistent with Tesoriero *et al* (2013) who suggested that watersheds in New England are less vulnerable to legacy groundwater N contamination than watersheds in the agricultural Midwest and urbanized east coast. Yet, heterogenous N concentrations in groundwater and apparent N attenuation within the aquifer suggest localized areas of groundwater N loading to streams are important locations for management (Mullaney and Schwarz 2013). Overall, the Farmington River watershed does not indicate watershed-wide groundwater N pollution and elevated N concentrations within the watershed are likely sourced from local and contemporary anthropogenic sources. Perhaps in New England watersheds, site (and even subsite) level understanding of groundwater N loading is particularly important when making management decisions. Our results indicate that nonpoint source N pollution from groundwater is driven by aquifer biogeochemistry and riparian forests within the river corridor which suggests that riparian buffers are helping to reduce, not only surface water N loading, but also N loading from groundwater sources (Mayer *et al* 2007). However, we also found elevated N concentrations in groundwater coinciding with little to no N attenuation which also suggests that some groundwater flowpaths are not effectively reducing N within riparian buffers (Hester and Fox 2020). Groundwater N loading is lagged in time behind surface water N

loading and will continue to confound surface water quality management from months to decades (Van Meter and Basu 2017). We suggest that watershed managers continue to mitigate N loading through wide riparian buffers and to be cautious when extrapolating nonpoint source groundwater N loading due to significant heterogeneity in where, and how much, groundwater N enters river networks.

5. Conclusion

Nitrogen concentrations in groundwater discharging to streams—along individual expressions of groundwater discharge, single stream reaches, and across the watershed—were highly heterogeneous, varying 20-fold along the mainstem. Although in this mixed land use watershed, we expected N application at the recharging land area to be a dominant predictor of the variation in N concentration in discharging groundwater, we found instead that the combined effects of groundwater chemistry, flowpath distance and flux rate, and riparian land cover best predicted N concentrations. This suggests that the predictability of N loading from land cover is obscured by reactivity along groundwater flow paths; interestingly, relatively high and variable DO and SO_4^{2-} paired with low DOC concentrations indicated NO_3^- production through nitrification, and removal through sulfur-based denitrification and incomplete denitrification. Our results show that in mixed land use watersheds groundwater is not a well-mixed system and that N loading from groundwater is highly heterogenous across space further complicating our understanding of how land cover influences groundwater biogeochemistry. The consequences of heterogeneous N delivery from groundwater discharge are particularly important for extrapolating and predicting how groundwater-delivered N loads contribute to watershed export. Improved understanding of the fate of nonpoint source loading to watersheds will benefit efforts to mitigate N loading downstream.

Data availability statements

The data that support the findings of this study are openly available at the following https://doi.org/10.5066/P941XKST (Moore *et al* 2023).

Acknowledgments

We acknowledge review comments from two anonymous reviewers and one USGS reviewer that substantially improved the manuscript. We would like to thank Fiona Liu for significant field and laboratory help as an undergraduate researcher. Any use of trade, firm, or product names is for descriptive purposes only and does not imply endorsement by the U.S. Government.

Ethical statement

No humans subjects were used in this research.

Funding Information

This research was funded by NSF-EAR Award Number 1824820 and USDA HATCH Project CONS00938.

Conflict of interest

The authors declare no conflict of interest

References

Barclay J R, Briggs M A, Moore E M, Starn J J, Hanson A E H and Helton A M 2022 Where groundwater seeps: evaluating modeled groundwater discharge patterns with thermal infrared surveys at the river-network scale *Adv. Water Resour.* **160** 104108

Barclay J R, Starn J J, Briggs M A and Helton A M 2020a Improved prediction of management-relevant groundwater discharge characteristics throughout river networks *Water Resour. Res.* **56** e2020WR028027

Barclay J, Starn J J, Briggs M and Helton A 2020b *MODFLOW-NWT and MODPATH Groundwater Flow Models of the Farmington River Watershed (Connecticut and Massachusetts)* (U.S. Geological Survey) (https://doi.org/10.5066/P960RSK)

Ben Maamar S, Aquilina L, Quaiser A, Pauwels H, Michon-Coudouel S, Vergnaud-Ayraud V and Dufresne A 2015 Groundwater isolation governs chemistry and microbial community structure along hydrologic flowpaths *Front. Microbiol.* **6** 1457

Böhlke J K, Wanty R, Tuttle M, Delin G and Landon M 2002 Denitrification in the recharge area and discharge area of a transient agricultural nitrate plume in a glacial outwash sand aquifer, Minnesota *Water Resour. Res.* **38** 10–11

Briggs M A and Hare D K 2018 Explicit consideration of preferential groundwater discharges as surface water ecosystem control points *Hydrol. Process.* **32** 2435–40

Briggs M A, Jackson K E, Liu F, Moore E M, Bisson A and Helton A M 2021 Exploring local riverbank sediment controls on the occurrence of preferential groundwater discharge points *Water* **14** 11

Byrnes D K, Van Meter K J and Basu N B 2020 Long-term shifts in U.S. nitrogen sources and sinks revealed by the new TREND-nitrogen data set (1930–2017) *Glob. Biogeochem. Cycles* **34** e2020GB006626

Chang S Y, Zhang Q, Byrnes D K, Basu N B and van Meter K J 2021 Chesapeake legacies: the importance of legacy nitrogen to improving Chesapeake Bay water quality *Environ. Res. Lett.* **16** 085002

Chen N, Wu J, Chen Z, Lu T and Wang L 2014 Spatial-temporal variation of dissolved N2 and denitrification in an agricultural river network, southeast China *Agric. Ecosyst. Environ.* **189** 1–10

Cole M L, Kroeger K D, McClelland J W and Valiela I 2006 Effects of watershed land use on nitrogen concentrations and δ15 nitrogen in groundwater *Biogeochemistry* **77** 199–215

Deitchman R S and Loheide S P 2009 Ground-based thermal imaging of groundwater flow processes at the seepage face *Geophys. Res. Lett.* **36** 14

Dewitz J U.S. Geological Survey 2021 National Land Cover Database (NLCD) 2019 Products *U.S. Geological Survey Data Release* (ver. 2.0, June 2021) 2.0

Dugdale S J, Bergeron N E and St-Hilaire A 2015 Spatial distribution of thermal refuges analysed in relation to

riverscape hydromorphology using airborne thermal infrared imagery *Remote Sens. Environ.* **160** 43–55
ESRI 2021 *ArcGIS Desktop: Release 10* (Environmental Systems Research Institute)
Fowler D, Coyle M, Skiba U, Sutton M A, Cape J N, Reis S and Voss M 2013 The global nitrogen cycle in the twenty-first century *Phil. Trans. R. Soc.* B **368** 20130164
Galloway J N and Cowling E B 2002 Reactive nitrogen and the world: 200 years of change *Ambio* **31** 64–71
Gorski G, Fisher A T, Dailey H, Beganskas S, Schmidt C and Galen Gorski C 2022 The potential for nitrate removal during infiltration: mapping with machine learning informed by field and laboratory experiments *Hydrol. Process.* **36** e14750
Hare D K, Boutt D F, Clement W P, Hatch C E, Davenport G and Hackman A 2017 Hydrogeological controls on spatial patterns of groundwater discharge in peatlands *Hydrol. Earth Syst. Sci.* **21** 6031–48
Harvey J and Wagener B 2000 Quantifying hydrologic interaction between streams and their subsurface hyporheic zones *Streams and Groundwaters* (Academic Press) pp 3–44
Hayakawa A, Ota H, Asano R, Murano H, Ishikawa Y and Takahashi T 2021 Sulfur-based denitrification in streambank subsoils in a headwater catchment underlain by marine sedimentary rocks in Akita, Japan *Front. Environ. Sci.* **9** 384
Haynes A B, Briggs M A, Moore E M, Jackson K E, Barclay J R and Helton A M 2023 Shallow and local or deep and regional? Inferring source groundwater characteristics across mainstem riverbank discharge faces *Hydrol. Process.* **37** e14939
Helton A M, Bernhardt E S and Fedders A 2014 Biogeochemical regime shifts in coastal landscapes: the contrasting effects of saltwater incursion and agricultural pollution on greenhouse gas emissions from a freshwater wetland *Biogeochemistry* **120** 133–47
Henri C V and Harter T 2022 Denitrification in heterogeneous aquifers: relevance of spatial variability and performance of homogenized parameters *Adv. Water Resour.* **164** 104168
Hester E T and Fox G A 2020 Preferential flow in riparian groundwater: gateways for watershed solute transport and implications for water quality management *Water Resour. Res.* **56** 12
Hinshaw S E, Zhang T, Harrison J A and Dahlgren R A 2020 Excess N_2 and denitrification in hyporheic porewaters and groundwaters of the San Joaquin River, California *Water Res.* **168** 115161
Houlton B Z and Morford S L 2014 The synthesis for terrestrial nitrogen inputs *Soil* **1** 381–7
Jackson K E, Haynes A B and Briggs M A 2023 *Passive seismic depth to bedrock data collected along streams of the Farmington River watershed, CT, USA* (U.S. Geological Survey data release) (https://doi.org/10.5066/P9FTZ0DK)
Jenkins E H 1925 A history of Connecticut agriculture *Free Download, Borrow, and Streaming: Internet Archive* (available at: https://archive.org/details/historyofconnect00jenk) (Accessed 14 December 2022) (Edward Hopkins), b. 1850
Johnson H M and Stets E G 2020 Nitrate in streams during winter low-flow conditions as an indicator of legacy nitrate *Water Resour. Res.* **56** e2019WR026996
Kaushal S S, Groffman P M, Band L E, Elliott E M, Shields C A and Kendall C 2011 Tracking nonpoint source nitrogen pollution in human-impacted watersheds *Environ. Sci. Technol.* **45** 8225–32
Kennedy C D, Genereux D P, Corbett D R and Mitasova H 2009 Relationships among groundwater age, denitrification, and the coupled groundwater and nitrogen fluxes through a streambed *Water Resour. Res.* **45** 9402
Kolbe T *et al* 2019 Stratification of reactivity determines nitrate removal in groundwater *Proc. Natl Acad. Sci. USA* **116** 2494–9
Lamberti G and Hauer F R 2017 *Methods in Stream Ecology: Volume 2: Ecosystem Function* (Elsevier Science)
Liu Y, Engel B A, Flanagan D C, Gitau M W, McMillan S K and Chaubey I 2017 A review on effectiveness of best management practices in improving hydrology and water quality: needs and opportunities *Sci. Total Environ.* **601–602** 580–93
Lockhart K M, King A M and Harter T 2013 Identifying sources of groundwater nitrate contamination in a large alluvial groundwater basin with highly diversified intensive agricultural production *J. Contam. Hydrol.* **151** 140–54
Lutz S R, Trauth N, Musolff A, Van Breukelen B M, Knöller K and Fleckenstein J H 2020 How important is denitrification in riparian zones? combining end-member mixing and isotope modeling to quantify nitrate removal from riparian groundwater *Water Resour. Res.* **56** e2019WR025528
Martin S L, Hamlin Q F, Kendall A D, Wan L and Hyndman D W 2021 The land use legacy effect: looking back to see a path forward to improve management *Environ. Res. Lett.* **16** 035005
Mayer P M, Reynolds S K, McCutchen M D and Canfield T J 2007 Meta-analysis of nitrogen removal in riparian buffers *J. Environ. Qual.* **36** 1172–80
McAleer E B, Coxon C E, Richards K G, Jahangir M M R, Grant J and Mellander P E 2017 Groundwater nitrate reduction versus dissolved gas production: a tale of two catchments *Sci. Total Environ.* **586** 372–89
Megonigal J P, Hines M E and Visscher P T 2003 Anaerobic metabolism: linkages to trace gases and aerobic processes *Treatise on Geochemistry* vol 8 ed William H S (Elsevier) pp 317–424
Moore E M, Haynes A B, Jackson K E, Bisson A M, Barclay J R, Liu F, Briggs M A and Helton A M 2023 Biogeochemical and source characteristics of preferential groundwater discharge in the Farmington River watershed (Connecticut and Massachusetts, 2017–2021): U.S *Geological Survey Data Release* (https://doi.org/10.5066/P941XKST)
Moore E M, Jackson K E, Haynes A B, Harvey M, Helton A M and Briggs M A 2020 Thermal infrared images of groundwater discharge zones in the Farmington and Housatonic River watersheds (Connecticut and Massachusetts, 2019) Ver. 2.0 (November 2021) (U.S. Geological Survey data release) (https://doi.org/10.5066/P915E8JY)
Mulholland P J, Helton A M, Poole G C, Hall R O, Hamilton S K, Peterson B J and Thomas S M 2008 Stream denitrification across biomes and its response to anthropogenic nitrate loading *Nature* **452** 202–5
Mullaney J R and Schwarz G E 2013 *Estimated nitrogen loads from selected tributaries in Connecticut draining to Long Island Sound, 1999–2009* Scientific Investigations Report 2013-5171 (U.S. Geological Survey) 10.3133/sir20135171
National Oceanic and Atmospheric Administration, Office for Coastal Management *Coastal Change Analysis Program (C-CAP) Regional Land Cover* (NOAA Office for Coastal Management) (available at: www.coast.noaa.gov/htdata/raster1/landcover/bulkdownload/30m_lc) (Accessed 10 2022)
Nauman T W, Thompson J A and Rasmussen C 2014 Semi-automated disaggregation of a conventional soil map using knowledge driven data mining and random forests in the Sonoran desert, USA *Photogramm. Eng. Remote Sens.* **80** 353–66
Niswonger R G, Panday S and Ibaraki M 2011 MODFLOW-NWT, A Newton formulation for MODFLOW-2005 *Tech. Methods* **6** 44
Ocampo C J, Oldham C E, Sivapalan M and Turner J V 2006 Hydrological versus biogeochemical controls on catchment nitrate export: a test of the flushing mechanism *Hydrol. Process.* **20** 4269–86
Olcott P G 1995 Connecticut, Maine, Massachusetts, New Hampshire, New York, Rhode Island, Vermont, HA 730-M *Groundwater Atlas of the US* (United States Geological Survey)
Pollock D W 2012 User guide for MODPATH version 6—A particle-tracking model for MODFLOW *Techniques and Methods* (https://doi.org/10.3133/TM6A41)

Puckett L J, Tesoriero A J and Dubrovsky N M 2011 Nitrogen contamination of surficial aquifers-A growing legacy *Environ. Sci. Technol.* **45** 839–44

R Core Team 2021 R: a language and environment for statistical computing *R Foundation for Statistical Computing, Vienna, Austria* (available at: www.R-project.org/)

Ranalli A J and Macalady D L 2010 The importance of the riparian zone and in-stream processes in nitrate attenuation in undisturbed and agricultural watersheds—A review of the scientific literature *J. Hydrol.* **389** 406–15

Reitz M, Sanford W E, Senay G B and Cazenas J 2017 Annual estimates of recharge, quick-flow runoff, and evapotranspiration for the contiguous U.S. Using empirical regression equations *J. Am. Water Resour. Assoc.* **53** 961–83

Rivett M O, Buss S R, Morgan P, Smith J W N and Bemment C D 2008 Nitrate attenuation in groundwater: a review of biogeochemical controlling processes *Water Res.* **42** 4215–32

Rosenberry D O, Briggs M A, Delin G and Hare D K 2016 Combined use of thermal methods and seepage meters to efficiently locate, quantify, and monitor focused groundwater discharge to a sand-bed stream *Water Resour. Res.* **52** 4486–503

Rosenberry D O, Engesgaard P and Hatch C 2021 Hydraulic conductivity can no longer be considered a fixed property when quantifying flow between groundwater and surface water *Hydrol. Process.* **35** e14226

Sanford W E and Pope J P 2013 Quantifying groundwater's role in delaying improvements to Chesapeake Bay water quality *Environ. Sci. Technol.* **47** 13330–8

Scanlon B R, Reedy R C, Stonestrom D A, Prudic D E and Dennehy K F 2005 Impact of land use and land cover change on groundwater recharge and quality in the southwestern US *Glob. Change Biol.* **11** 1577–93

Shabaga J A and Hill A R 2010 Groundwater-fed surface flow path hydrodynamics and nitrate removal in three riparian zones in southern Ontario, Canada *J. Hydrol.* **388** 52–64

Stets E G, Sprague L A, Oelsner G P, Johnson H M, Murphy J C, Ryberg K and Riskin M L 2020 Landscape drivers of dynamic change in water quality of U.S. rivers *Environ. Sci. Technol.* **54** 4336–43

Sullivan C J, Vokoun J C, Helton A M and Briggs M A 2021 An ecohydrological typology for thermal refuges in streams and rivers *Ecohydrology* **14** e2295

Tesoriero A J, Duff J H, Saad D A, Spahr N E and Wolock D M 2013 Vulnerability of streams to legacy nitrate sources *Environ. Sci. Technol.* **47** 3623–9

Tesoriero A J, Liebscher H and Cox S E 2000 Mechanism and rate of denitrification in an agricultural watershed: electron and mass balance along groundwater flow paths *Water Resour. Res.* **36** 1545–59

Tesoriero A J, Stratton L E and Miller M P 2021 Influence of redox gradients on nitrate transport from the landscape to groundwater and streams *Sci. Total Environ.* **800** 150200

U. S. Census Bureau 1990 TIGER/line data (available at: www.census.gov/data/data-tools.html)

U. S. Geological Survey 2023 National Water Information System (available at: http://waterdata.usgs.gov/nwis/) (Accessed 1 February 2023)

Van Meter K J and Basu N B 2017 Time lags in watershed-scale nutrient transport: an exploration of dominant controls *Environ. Res. Lett.* **12** 084017

Van Meter K J, Van Cappellen P and Basu N B 2018 Legacy nitrogen may prevent achievement of water quality goals in the Gulf of Mexico *Science* **360** 427–30

Vero S E, Basu N B, Van Meter K, Richards K G, Mellander P E, Healy M G and Fenton O 2018 Revue: L'état environnemental et les implications du décalage temporel du nitrate en Europe et Amérique du Nord *Hydrogeol. J.* **26** 7–22

Ward B B 2008 Nitrification *Encyclopedia of Ecology, Five-Volume Set* (Academic Press) pp 2511–8

Wherry S A, Tesoriero A J and Terziotti S 2021 Factors affecting nitrate concentrations in stream base flow *Environ. Sci. Technol.* **55** 902–11

Winter T C, Harvey J W, Franke O L and Alley W M 1998 *Ground Water and Surface Water-a Single Resourcex* (U.S. Geological Survey) Circular 1139

Wollheim W M, Vörösmarty C J, Peterson B J, Seitzinger S P and Hopkinson C S 2006 Relationship between river size and nutrient removal *Geophys. Res. Lett.* **33**